Proceedings of the International Association for
Shell and Spatial Structures (IASS) Symposium 2013
„BEYOND THE LIMITS OF MAN"
23-27 September, Wroclaw University of Technology, Poland
J.B. Obrębski and R. Tarczewski (eds.)

GRAPHICAL STATICS AND MAXWELL'S THEOREM APPLIED TO AN ELEMENTARY BRANCHING STRUCTURE

Edmond Saliklis[1], Jonas Houston[2]

[1]Associate Professor, Dept. of Architectural Engineering, California Polytechnic State Univ., San Luis Obispo, CA, USA, *esalikli@calpoly.edu*
[2] Sr. Designer, Nabih Youssef & Associates, San Francisco, California,USA *jonashouston2@yahoo.com*

Summary: The coupling of design and analysis through the use of graphical statics is demonstrated and bolstered by the introduction of Maxwell's Theorem in the design loop. This process is shown through the manipulation of a branching structure, also known as a dendriform. The example structure is purposely kept simple to demonstrate the process, which includes a brief overview of graphical statics.

Keywords: *Graphical statics, Maxwell's theorem, Dendriform, Branching Structures, Structural Design*

1. INTRODUCTION

The purpose of this paper is to revisit a two dimensional truss structural form known as a branching structure or architectural dendriform, to highlight the powerful but often overlooked Maxwell's Theorem as a means of gaining structural insights and finally to champion the recent resurgence of graphical statics as a pedagogical and design/analysis tool. A brief review of graphical statics principles will be followed by a demonstrative exercise that highlights the ideas of linking graphical statics to Maxwell's Theorem to gain design insights.

Recently (Mauer 1998, Gerhardt 2003, Block 2006) several researchers have summarized the historical arc taken by graphical statics both in academia and in practice. Two recent textbooks (Zalewski 1998, Allen 2010])have contributed greatly to the resurgence of graphical statics and they have spawned a new body of work that elegantly combines the classical graphical method with state-of-the art computer graphics and sophisticated mathematical theories [Block 2007, De Lorenzis 2008].

The reader is encouraged to review these papers as well as the seminal primary sources which are now readily available in digital format for free on the internet and as paperback reprints of the original texts (Cremona 1890, Wolfe 1928).

2. REVIEW OF FORCE POLYGON AND FORM POLYGON CONSTRUCTION GRAPHICALLY

The fact that the polygon of force vectors and the assemblage of geometric lines forming a funicular shape corresponding to those force vectors are interchangeable, or reciprocal has been the basis of graphical statics since the earliest works on the subject. In this paper, we choose to explore a two dimensional structural form called a dendriform, also known as a branching structure. Branching structures have been studied extensively by Frei Otto in the Institute for Lightweight structures since the 1960s (Otto 1995) in a search for minimal structures that successfully carry a prescribed load. The work of the Institute (IL) elegantly combined experimental studies of branching structures with computer generated graphical studies. Others (von Buelow 2007) have studied form finding of branching structures through the prism of genetic algorithms. A unique approach to studying this form is to analyze it using graphical statics as was done in Allen's recent textbook (Allen 2010). In this paper, the graphical statics approach has been linked to Maxwell's Theorem to provide a new informative way of form finding.

For any statically determinate structure, the force polygon can be defined as the projected geometry of the form polygon and vice versa. Because of this interdependency between the form and force polygons, an entirely new structural form can be achieved by altering the associated force polygon.

The branching structure is chosen for study here because it is a curious yet extremely efficient truss-like structure. Designers wishing to control the forces in structural members can make adjustments on the force polygon, and see the corresponding form polygon immediately. A three tiered branching structure supporting a uniform horizontal roof load is shown in Figure 1.

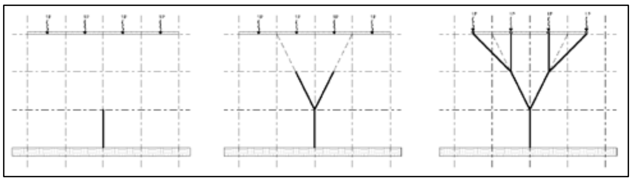

Fig. 1. Creating the branching structure

The lowest tier must point to the centroid of all of the roof loads. One could choose any number of branches for the second tier, here the structure splits into two branches, and the trajectory of each second tier branch points at the centroid of the portion of the roof load that it is responsible for. Finally, the third tier splits into some arbitrary number of branches again, here into two, with each of the third tier branches pointing to the centroid of the portion of the roof load assigned to it. In the rightmost image of Figure 1, notice that the monolithic roof has been changed to a series of pin-ended two force members.

Having established the geometry of this compression-only branching structure with a roof plate experiencing tension it is worth noting that the structure is indeed stable for these loads despite the quadrilateral interior panel. Thus the entire structure can be classified as a funicular geometry for the given loads. Now one can use Bow's notation as shown in Figure 2 wherein capital letters are placed between the loads and numbers are placed in interior panels.

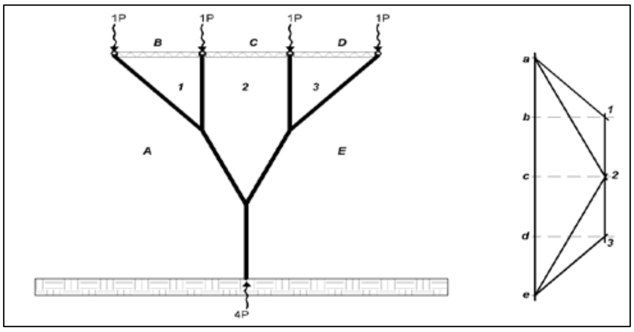

Fig. 2. Original form and force polygons

This allows the force polygon to be established using lower case letters and numbers at any convenient scale. In the force polygon, vector ab is a vertical downward drop of 1P, drawn to the chosen scale, because it captures the vertical downward load from A to B on the form polygon. Similarly on the force polygon vectors bc, cd and de all capture the corresponding downward external loads shown on the form polygon. The vector ea represents the vertical upward reaction of 4P ensuring global equilibrium of the external forces/reaction system. The force in each branch of the structure can be found by projecting parallel lines that locate each number sequentially. Establishing point 1 on the force polygon requires drawing a line parallel to branch A1 (or 1A) through point a and a line parallel to roof segment B1 (or 1B) through point b. The intersection of these two lines on the force polygon uniquely identifies point 1. Measuring the length of the line at the chosen scale spanning from a to 1 (or 1 to a) establishes the magnitude of the force in that branch of the structure.

To demonstrate the design/analysis loop, suppose the designer was interested in lowering the force in the third tier branch A1 (or 1A) by 15% and simultaneously the designer was willing to increase the force in the third tier branch 3E (or E3) by 15%. Using the scale already chosen for the force polygon, the designer would move point 1 horizontally to the left in the force polygon (horizontally because the slope of the roof is not allowed to change in this particular re-design example) and point 3 would move horizontally to the right till the desired forces are reached. The modified geometry of the force polygon can be seen in Figure 3 which shows how nodes 1 and 2 were adjusted.

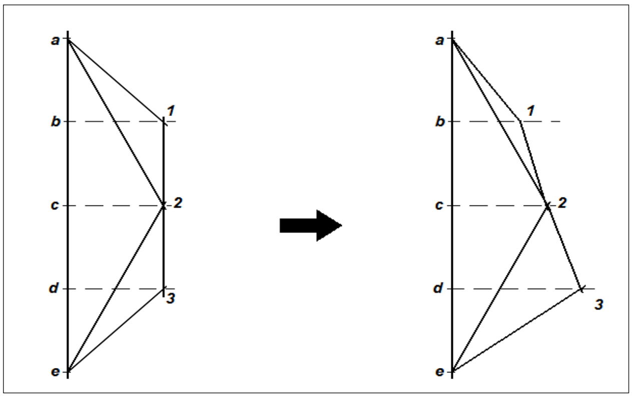

Fig. 3: Altered geometry of force polygon

Having established the new force polygon, a corresponding geometry for the branching structure must be defined. In this example, the choice to modify the exterior branch forces A1 and E3 called for the movements of points 1 and 3. But as seen in Figure 3, the vectors a1, 12, 23 and 3e have all been affected by this re-design. Yet since point 2 was not shifted in Figure 3, then the second tier forces a2 and 2e and the corresponding second tier branches A2 and 2E were not affected, nor was the trunk AE affected. The new geometry of the structure can be found by projecting the changes of the force polygon onto the form polygon. This is readily accomplished since the geometry of the first and second tier branches did not change, the new third tier geometries originate at the top of the second tier. The resulting branching structure can be seen in Figure 4 with dashed lines denoting the previous location of the branches of the original form.

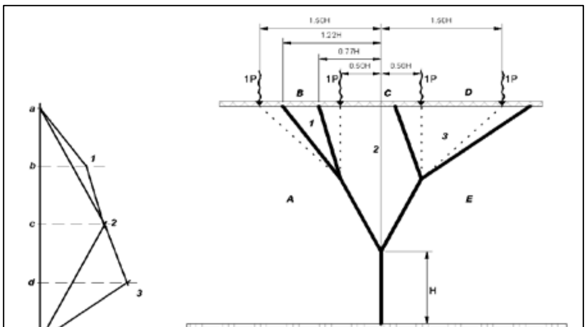

Fig. 4: New Structure due to changes in Force Polygon

2.1. The External Loads Reconsidered

After attaining the new form, it is clear that the external vertical loads of the roof are not applied at the joints, violating the well-known rule for loading pin-ended two force members only at the joints. To rectify this, the original external loading must be placed at the top nodes of the top tier branches as shown in Figure 5.

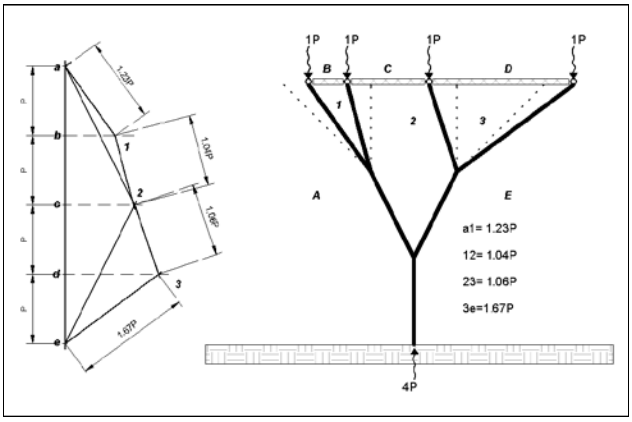

Fig. 5: Moved but Equivalent External Loading

At first glance it may seem that now the problem has changed, but verification that the loads on the roof of Figure 4 are indeed statically equivalent to the loads on the roof of Figure 5 can be achieved by summing their effective moments about an arbitrary point. The two loading patterns give identical moments. The static equivalency of the external loads in Figures 4 and 5 calls to mind the powerful, yet often overlooked Maxwell's Theorem. Begin by noting that the third tier branch forces have changed as desired, with member A1 experiencing the planned 15% decrease and member 3E the 15% increase in axial load. The forces in the roof elements B1 and D3 are also affected by this new design.

2.2. Insight from Maxwell's Theorem

Maxwell's Theorem (Baker, 2012) is explicated beautifully in the reciprocal geometries that form the core of graphical statics. The theorem equates the internal and external energy in a truss as shown in equations 1 and 2:

Internal Energy = External Energy (1)

$$\Sigma F_i L_i = \Sigma \vec{P}_i \bullet \vec{r}_i \,, \qquad (2)$$

where F_i is the internal axial force of member i,

L_i is the length of member i,

$\vec{P}_i$ is the vector of the i^{th} external force with respect to a global coordinate system, and

$\vec{r}_i$ the vector defining the location of that external force with respect to the origin of the coordinate system.

Note that the right hand side of the equation is a dot product causing the right hand side to be a scalar. The internal work can be broken into two parts consisting of internal energy due to tension members and internal energy due to compression members as seen in equation 3.

$$\left[\Sigma F_i L_i\right]_{tension} - \left[\Sigma F_i L_i\right]_{compression} = \Sigma \vec{P}_i \bullet \vec{r}_i \qquad [3]$$

Next assume that a design criterion exists such that the designer wants each member of the structure to produce some predetermined prescribed stress regardless of the force it is subjected to, then using the axial stress equation,

$$F_i = \sigma_{prescribed} * A_i \qquad [4]$$

where

$\sigma_{prescribed}$ is the prescribed axial stress (tension and compression),

A_i is the cross sectional area of member i, and

F_i is the internal force of member i as defined previously,

equation 4 can be substituted into equation 3,

$$\left[\Sigma \sigma_{presc} * A_i L_i\right]_{tension} - \left[\Sigma \sigma_{presc} * A_i L_i\right]_{compression} = \Sigma \vec{P}_i \bullet \vec{r}_i \qquad [5]$$

Inspection of equation 5 shows that an embedded volume term exists in the form of the product of A_i and L_i. Replacing that product with the variable V_i representing the volume of member i, equation 5 becomes

$$\left[\Sigma \sigma_{prescribed} * V_i\right]_{tension} - \left[\Sigma \sigma_{prescribed} * V_i\right]_{compression} = \Sigma \vec{P}_i \bullet \vec{r}_i \qquad [6]$$

The implication of the equations 3, 5 and 6 is that no matter the change in branching structure geometry, conservation of energy exists for a given set of external loads. If the external loading remains constant, that is if the right hand side of equation 6 does not change, then changes in the internal arrangement of the tension and compression elements in the truss (the left hand side of equation 6) always results in a constant number, regardless of the changes. Conservation of energy is preserved through a balancing of changes made to tension and compression members that comprise the internal energy. Figure 6 shows the various components that make up Maxwell's Theorem for the original form.

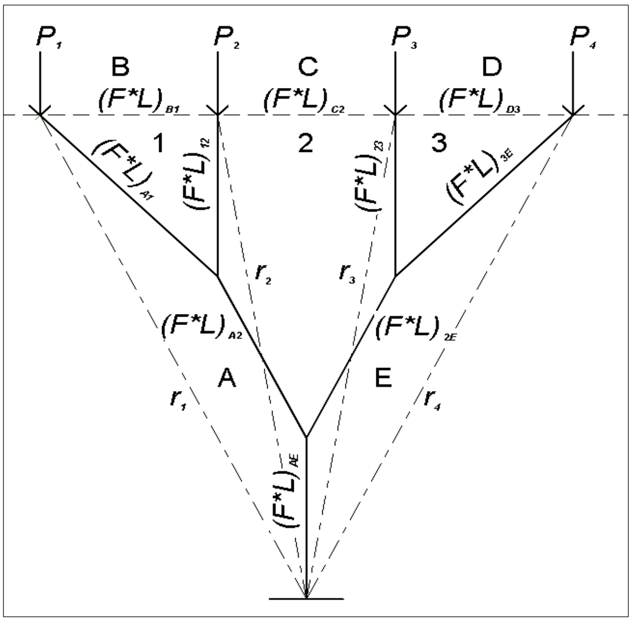

Fig. 6: Components of Maxwell's Theorem for Original Form

One design insight gained from the application of Maxwell's Theorem is the quest for convergence upon an optimum structure. Here optimum is defined as the creation of a structure from a minimum amount of material with all elements equally stressed to some prescribed value. Such a least volume structure would by this definition, be the optimum structure for a given set of loads. Maxwell's Theorem includes such a volume term and therefore allows for the tracking of a structure's efficiency based on the volume of equally stressed elements. An efficiency term is calculated as the net internal energy or the summation of the absolute values of each of the bracketed terms on the left hand side of equation 6.

$$\left|\left(\Sigma \sigma_{prescribed} * V\right)\right|_{tension} + \left|\left(\Sigma \sigma_{prescribed} * V\right)\right|_{compression} = \textit{Net Internal Energy} \qquad [7]$$

Minimizing the sum would be the most efficient structure. Absolute values of the tension and compression terms on the left hand side of equation 6 are needed to identify progress towards optimization otherwise a progression is not apparent because the sum of the positive and negative terms on the left hand side of equation 6 will always be a constant, as previously described.

To investigate the design implications of Maxwell's Theorem, a study of the absolute value terms of the left hand side of equation 6 was conducted for four forms of contrasting geometry. The four dendriforms and their respective force polygons can be seen in Figures 7, 8, 9 and 10. Where lengths are not given, symmetry about the vertical axis can be used. Form 1 is the original branching structure, **Form 4** is the modified structure that induced a 15% change of force in two branches. **Forms 2 and 3** used the described procedure of modifying the force polygon and extracting the resulting new form polygon.

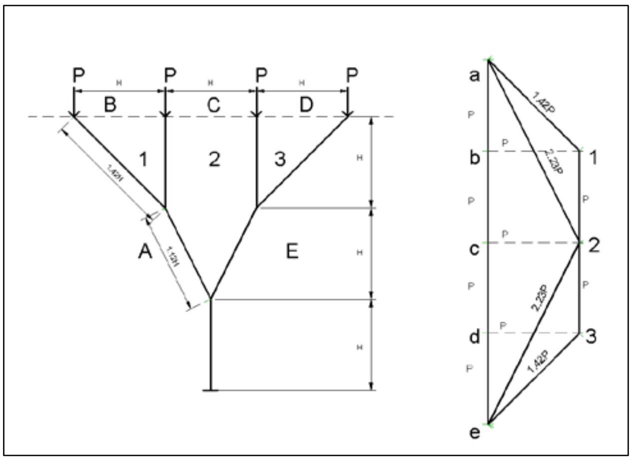

Fig. 7: Form 1 used for Maxwell Study

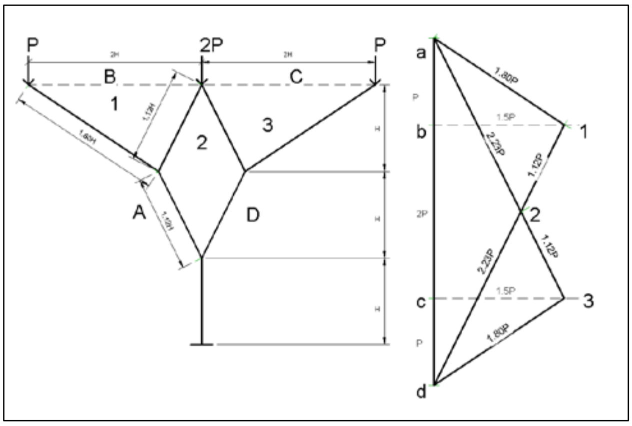

Fig. 8: Form 2 used for Maxwell Study

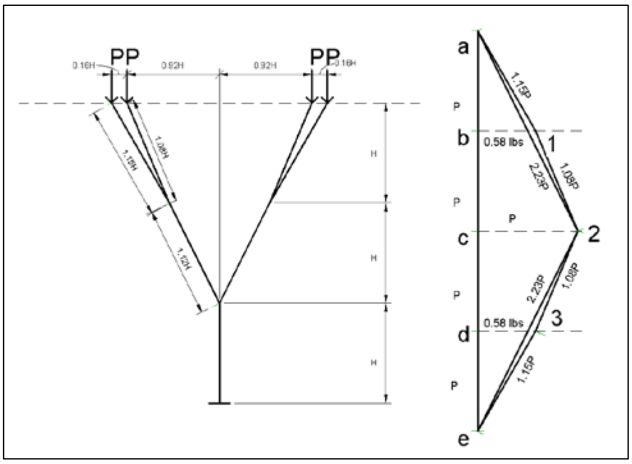

Fig. 9: Form 3 used for Maxwell Study

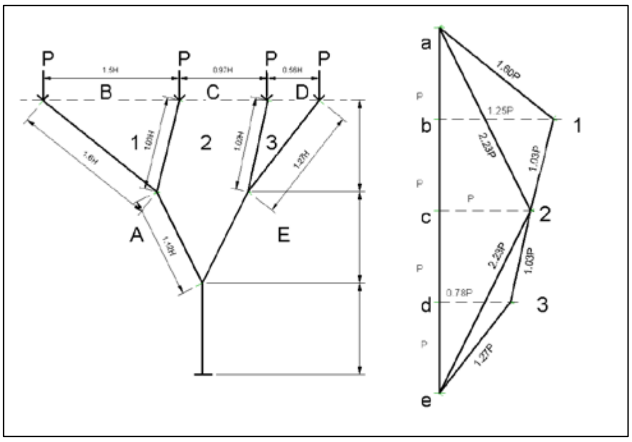

Fig. 10: Form 4 used for Maxwell Study

An example calculation of Maxwell's Theorem for Form 1 of Figure 7 will use the dimensionless force value P. The tensile values of the left hand side of equation 3 are;

$$\Sigma\left[F_i L_i\right]_{tension} = \left(FL\right)_{B1} + \left(FL\right)_{C2} + \left(FL\right)_{D3} =$$

$$(1P \cdot H + 1P \cdot H + 1P \cdot H) = 3PH \qquad [7]$$

Symmetry of Form 1 in Figure 7 allows for doubling of the second and third tier branches when calculating the compression components of the left hand side of Equation 3

$$\Sigma\left[F_i L_i\right]_{compression} = 2*\left[\left(FL\right)_{A1} + \left(FL\right)_{12} + \left(FL\right)_{A2}\right] + \left(FL\right)_{AE} \qquad Eqn\,8a$$

$$= 2\left[\left(1.42P \cdot 1.42H\right) + \left(P \cdot H\right) + \left(2.23P \cdot 1.12H\right)\right] + \left(4P \cdot H\right) = -15Ph \qquad Eqn\,8b$$

Note that compression is considered to be negative. Now the proposed efficiency term described earlier in this section can be found by adding the absolute values of the tension and compression force product summations, and the internal energy uses the same terms but without the absolute values.

$$Efficiency\ \ 1 = \left[\Sigma F_i L_i\right]_{tension} - \left[\Sigma F_i L_i\right]_{compression} = \left|3PH\right| + \left|-15PH\right| = 18PH \qquad [9]$$

$$\left[\Sigma F_i L_i\right]_{tension} - \left[\Sigma F_i L_i\right]_{compression} = 3PH + \left(-15Ph\right) = -12PH \qquad [10]$$

The right hand side of Equation 3 is the external energy and is calculated below.

$$\Sigma \vec{P}_i \bullet \vec{r}_i$$

$$= \begin{Bmatrix} 0 \\ -1 \end{Bmatrix} \bullet \begin{Bmatrix} -1.5 \\ 3 \end{Bmatrix} + \begin{Bmatrix} 0 \\ -1 \end{Bmatrix} \bullet \begin{Bmatrix} -0.5 \\ 3 \end{Bmatrix} + \begin{Bmatrix} 0 \\ -1 \end{Bmatrix} \bullet \begin{Bmatrix} 0.5 \\ 3 \end{Bmatrix} + \begin{Bmatrix} 0 \\ -1 \end{Bmatrix} \bullet \begin{Bmatrix} 1.5 \\ 3 \end{Bmatrix}$$

$$= -12PH \qquad\qquad Eqn\quad 11$$

It can be seen that the summation of internal and external energy is equal to zero, or that the right hand side of Maxwell's Theorem is equal to the left hand side. For this particular loading, the constant will always equal -12PH. Closer inspection of the dot product of this loading case reveals that the horizontal components will always equal zero because the loading is strictly in the vertical axis, the horizontal component of load is zero thus changes in the horizontal component of the radial vector $\vec{r}_i$ have no effect on the dot product calculation. This explains why shifting the loads laterally from Figure 4 to Figure 5 produced a statically equivalent condition.

To gain further insight of the changes to this elementary branching structure, an overall stiffness was captured as the average vertical movement of the roof joints for each of the four forms. Also the total weight of each form was tracked. Recall that cross sections of members were varied to ensure that each member experienced the same constant prescribed stress. The length of each element was multiplied by the required cross sectional area to get a volume, and the volume was given some density. Table 1 below summarizes the results.

TABLE 1. Summary of Results

Ranked by Increasing Stiffness				FORM	Ranked by Decreasing Weight				FORM
	1.509259	596.577	Stretched	2		**-0.00543**	1.333032	Stretched	2
	1.027778	467.522	Unsymm	4		**-0.0037**	1.044663	Unsymm	4
	1	447.534	Original	1		**-0.0036**	1	Original	1
	0.819444	447.332	Pinched	3		**-0.00295**	0.999549	Pinched	3

2.3. Insights

Ranking the four branching structures according to any of the varying Maxwell's Theorem's terms that shows consistent progress, the individual energy terms decrease, the net internal energy decreases, the stiffness increases and the weight decreases. The only exception is the stiffness of Form 4, and this is an artifact of the method used to arrive at an "average" stiffness. A final finding comes from comparing the first two rows of Table 1 where it is seen that the designer gets penalized twice when diverging from the optimum structure; one penalty due to the tension members and another penalty for the compression members.

3. CONCLUSIONS

The investigation of Maxwell's Theorem can be adapted to various structures and can give insight into structural efficiency. When paired with target structural goals such stiffness and minimal weight, Maxwell's Theorem can help develop parametric studies with the goal of arriving at a structurally sound solution. Such parametric studies would be fascinating to conduct in current digital form finding tools such as RhinoScript and Grasshopper.

4. REFERENCES

[1] Allen, E. and Zalewski, W. and (2010), Form and Forces, John Wiley & Sons, New York.

[2] Baker, W., Beghini, A., Mazurek, A. (2012). "Applications of Structural Optimization in Architectural Design." Proceedings of the Structures Congress 2012, 20th Analysis and Computation Specialty Conference, pp. 257 – 266

[3] Block, P., DeJong, M. and Ochsendorf, J. (2006), As hangs the chain, Nexus Network Journal Vol. 8, No. 2, pp 13- 24.

[4] Block, P. and Ochsendorf, J. (2007). Thrust Network Analysis: A New Methodology for Three-dimensional Equilibrium, Journal of the International Association for Shell and Spatial Structures 48(3), 167-173.

[5] Cremona, L. (1890 and as Google Book) Graphical statics; two treatises on the graphical calculus and reciprocal figures in graphical statics.

[6] De Lorenzis, L., and Ochsendorf, J., Failure of Rectangular Buttress under Concentrated Loading, Journal of Structures and Buildings, Institution of Civil Engineers, Vol. 161, No. 5, pp. 265-275, October 2008.

[7] Gerhardt, R., Kurrer, K. and Pichler, G. (2003), The methods of graphical statics and their relation to the structural form, Proceedings of the First International Congress on Construction History, Madrid, pp 997-1006.

[8] Maurer, B. (1998) Karl Culmann und die graphische Statik, Berlin/Diepholtz/Stuttgart: Verlag fur die Geschichte der Naturwissenschaft und der Technik.

[9] Otto, F and Rasch, B. (1995) Frei Otto and Bodo Rasch, Finding Form. Towards an Architecture of the Minimal. Edition Axel Menges, pp. 157-165.

[10] Von Buelow, P. (2007) A Geometric Comparison of Branching Structures in Tension and Compression Versus Minimal Paths, proceedings of Shell and Spatial Structures, Structural Architecture, Venice, Italy, Dec. 3-6.

[11] Wolfe, W. (1921 and as Google Book) Graphical Analysis; a Text Book on Graphic Statics.

[12] Zalewski, W. and Allen, E. (1998), Shaping Structures Statics, John Wiley & Sons, New York.